Energy Conversion and Management 127 (2016) 355–365

Contents lists available at ScienceDirect

Energy Conversion and Management

journal homepage: www.elsevier.com/locate/enconman

Parametric investigations to enhance thermal performance of paraffin through a novel geometrical configuration of shell and tube latent thermal storage system

Zakir Khan *, Zulfiqar Khan, Kamran Tabeshf

Bournemouth University, Faculty of Science and Technology, NanoCorr, Energy and Modelling (NCEM), Fern Barrow, Talbot Campus, Poole, Dorset BH12 5BB, UK

ARTICLE INFO

Article history:
Received 1 July 2016
Received in revised form 23 August 2016
Accepted 8 September 2016
Available online 14 September 2016

Keywords:
Latent heat storage
Phase change material
Thermal conductivity
Heat transfer
Shell and tube

ABSTRACT

This paper presents a two-dimensional finite element computational model which investigates thermal behaviour of a novel geometrical configuration of shell and tube based latent heat storage (LHS) system. Commercial grade paraffin is used as a phase change material (PCM) with water is employed as a heat transfer fluid (HTF). In this numerical analysis, the parametric investigations are conducted to identify the enhancement in melting rate and thermal storage capacity. The parametric investigations are comprised of number and orientation of tube passes in the shell, longitudinal fins length and thickness, materials for shell, tube and fins, and inlet temperature of HTF. Numerical analysis revealed that the melting rate is significantly enhanced by increasing the number of tube passes from 9 to 21. In 21 passes configuration, conduction heat transfer is the dominant and effective mode of heat transfer. The length of fins has profound impact on melting rate as compared to fins thickness. Also, the reduction in thermal storage capacity due to an increase in fins length is minimal to that of increase in fins thickness. The influence of several materials for shell, tube and fins are examined. Due to higher thermal conductivity, the melting rate for copper and aluminium is significantly higher than steel AISI 4340, cast iron, tin and nickel. Similarly, the thermal storage capacity and melting rate of LHS system is increased by a fraction of 18.06% and 68.8% as the inlet temperature of HTF is increased from 323.15 K to 343.15 K, respectively. This study presents an insight into how to augment the thermal behaviour of paraffin based LHS system and ultimately, these findings inform novel design solutions for wide-ranging practical utilisation in both domestic and commercial heat storage applications.

1. Introduction

For a long era, the world energy requirements are served and assisted by fossil fuels. However, due to the number of downsides of using fossil fuels such as limited and depleting resources, inconsistent prices and emission of harmful gases have encouraged scientists and engineers to progress in technologies to take advantages of renewable energy. In order to respond to the unpredictable and fluctuating nature of renewable energy sources, latent heat storage (LHS) system provides a viable option. LHS utilises PCM to store surplus thermal energy within solar systems or heat recovery systems and retrieves it when needed, in order to minimise the gap between energy demand and supply [1,2].

However, due to low thermal conductivity of PCM, rapid energy storage and discharge has been a major obstacle. Therefore, LHS system requires a sensitive and responsive thermal energy storing and discharging technique. A significant body literature is available that deals with the enhancement of LHS system such as geometric orientations of LHS system [3,4], utilising extended surfaces [5,6], encapsulation of PCM [7–11], employing form stable PCM [12–17] and inclusion of high thermal conductivity additives to PCM [18–20].

To develop efficient and productive LHS systems, thermal behaviour of several configurations and orientations have been examined. PCMs are normally employed in rectangular, spherical, cylindrical and shell and tubes containers. Kamkari and Shokouhmand [21] conducted an experimental study to identify the effect of number of fins on heat transfer and melting rate of PCM in rectangular container. It was deducted that melting time for one fin and 3 fins were reduced by 18% and 37% as compared to without fins enclosure. However, an increase in number of fins resulted in

* Corresponding author.
E-mail addresses: zkhan2@bournemouth.ac.uk (Z. Khan), zkhan@bournemouth.ac.uk (Z. Khan), KTabeshf@bournemouth.ac.uk (K. Tabeshf).

http://dx.doi.org/10.1016/j.enconman.2016.09.030
0196-8904/

Nomenclature

C_p	specific heat at constant pressure (kJ/kg K)
F	volume force (Pa/m)
f	fraction of PCM in solid and liquid phase
f_s	fraction of PCM in solid phase
f_l	fraction of PCM in liquid phase
g	gravitational acceleration (m/s^2)
H	specific enthalpy (MJ)
k	thermal conductivity (W/m K)
L	latent heat of fusion (kJ/kg)
T	temperature of PCM (K)
T_s	temperature of solid region of PCM (K)
T_l	temperature of liquid region of PCM (K)
T_{pc}	phase change temperature (K)
p	pressure (Pa)
q	heat source term (W/m^3)
S	momentum source term
u	velocity (m/s)
α	small constant value
β	coefficient of thermal expansion (1/K)
κ	morphology constant of mushy zone
ρ	density (kg/m^3)
μ	dynamic viscosity (kg/m s)

Subscripts

s	solid phase of PCM
l	liquid phase of PCM

Acronyms

HTF	heat transfer fluid
LHS	latent heat storage
PCM	phase change material

reduced natural convection and thus the overall heat transfer rate was compromised. Kalbasi and Salimpour [22] numerically studied the impact of length and number of longitudinal fins on thermal performance of PCM in rectangular enclosure. It was reported that higher number of longitudinal fins with shorter length showed augmented natural convection as compared to few fins with longer length. It was recommended that an optimum value for fins length and number should be identified to optimise the system. On the contrary, Ren and Chan [23] reported that an increase in longitudinal fins length enhanced the melting rate of PCM and therefore small number of lengthy fins exhibited effective thermal performance as compared to large number of shorter fins.

Li and Wu [24] numerically investigated the influence of six longitudinal fins on melting rate of $NaNO_3$ in horizontal concentric tube. It was observed that extended fins can reduce the melting and solidification time by at least 14% compared to concentric tubes without fins. Darzi et al. [25] simulated the effect of number fins on melting and solidification rate of N-eicosane in horizontal concentric tube. It was noticed that melting time for 4, 10, 15 and 20 fins were reduced by 39%, 73%, 78% and 82% as compared to no fins case, respectively. Likewise, the solidification time was decreased by 28%, 62%, 75% and 85% as compared to no fins case, respectively. However, as an increase in fins number restrained natural convection, thus increase in fins presented more prominent influence on solidification than melting rate. Yuan et al. [26] simulated the impact of fins angle on melting rate of lauric acid in horizontal concentric tube. It was reported that fins angle plays a significant role in influencing melting rate. The different angles for installation of two fins were 0°, 30°, 45° and 90°. The melting rate for fins angle 0° was comparatively higher. Moreover, in case of fins angle 0°, an increase in inlet temperature of HTF from 60 °C to 80 °C reduced melting time by 59.24%.

Caron-Soupart et al. [27] conducted an experimental examination to identify the effect of vertical concentric tube orientations on melting rate, heat exchange power and storage density. Selected concentric tube orientations were consisted of a single HTF tube without fins, with longitudinal fins and with circular fins. It was noticed that the melting rate for tube with longitudinal fins and circular fins was significantly higher than that of the tube without fins. Likewise, the heat exchange power was increased by a factor of 10 for the fins orientations than without fins. However, due to provision of higher PCM volume, the tube without fins orientation exhibited higher thermal storage density. Likewise, Agyenim et al. [28] conducted an experimental investigation to identify the thermal response of erythritol as a PCM in three orientations of horizontal concentric tube. The three orientations were concentric tube with no fins, with circular fins and with longitudinal fins. It was noticed that after 8 h of charging, only longitudinal fins orientation was able to melt the entire PCM. Also, cumulative thermal energy storage for longitudinal fins was comparatively higher. During solidification process, longitudinal fins showed better thermal performance with reduced subcooling.

Rathod and Banerjee [29] experimentally evaluated the effect of three longitudinal fins on melting and solidification rate of stearic acid in shell and tube container. It was noticed that melting and solidification time was reduced by 24.52% and 43.6% as compared to without fins case, respectively. Luo et al. [30] numerically studied the impact of number of HTF tubes and their orientations in shell and tube container on thermal performance. It was observed that the required melting time for single HTF tube was 2.5 and 5 times than four and nine HTF tubes, respectively. Similarly, the thermal performance of centrosymmetric orientation is better than staggered and inline orientation. Esapour et al. [31] also examined the influence of number of HTF tubes in shell and tube container. It was noticed that by increasing the number of HTF tubes from 1 to 4, the melting time can be reduced by 29%. Therefore, it is evident that the number of HTF tubes has a good influence on thermal behaviour of LHS system.

Vyshak and Jilani [32] conducted a numerical study to compare the impact of rectangular, cylindrical, and shell and tube container orientations on melting rate of PCM. It was observed that for the same volume and heat transfer surface area, the melting rate for shell and tube configuration was comparatively higher.

Tao et al. [33] numerically investigated the influence of HTF tube geometry on melting time. The tested configurations involved smooth, dimpled, cone-finned and helical-finned tubes. It was reported that the melting time for dimple, cone-finned and helical-finned tube was reduced by 19.9%, 26.9% and 30.7% comparing to smooth tube, respectively. Likewise, Li et al. [34] reported that heat transfer rate can be significantly enhanced by employing internally ribbed tubes instead of smooth tubes. Furthermore, the influence of the numbers, geometrical configurations and orientations of fins on thermal behaviour of LHS system is discussed in [35–40].

The mass flow rate of HTF has a minimal influence on thermal behaviour as compared to inlet temperature of HTF and geometrical configuration of LHS system. Seddegh et al. [41] numerically examined the influence of vertical and horizontal orientation of

shell and tube container on thermal behaviour of LHS system. Moreover, it was noticed that mass flow rate of HTF has insignificant influence on melting rate. Kibria et al. [42] conducted numerical and experimental examination of paraffin wax in shell and tube container. It was deduced that mass flow rate of HTF has negligible effect on thermal performance. Also, Wang et al. [43] numerically investigated the enhancement in thermal performance of shell and tube container due to inlet temperature and mass flow rate of HTF. It was observed that the inlet temperature has more profound impact on melting rate and thermal storage capacity than mass flow rate of HTF. Thus, this article will not consider the parametric investigation of mass flow rate of HTF.

In this article, the parametric investigation of a novel geometrical configuration of a shell and tube model is conducted. This specific orientation of shell and tube with longitudinal fins has not been reported in literature. A two-dimensional computational model is applied to a novel shell and tube configuration. This article is focused on identifying the influence of number of tube passes and their orientation in the shell on the melting rate and thermal storage capacity. Moreover, the parametric investigations of fins length, fins thickness and materials for shell, tubes and fins are conducted to investigate the impact on thermal behaviour of LHS system. The influence of inlet temperature of HTF on melting rate and thermal storage capacity is also examined. This article will help in highlighting the parameters that can enhance the thermal performance of LHS system and therefore, the large scale practical utilisation in various domestic and industrial applications, time-saving and economic benefits can be achieved.

2. Numerical model

2.1. Physical model

Physical configuration of LHS system is presented in Fig. 1. Parametric investigations of novel shell and tube model has been conducted to address the enhancement of phase transition rate and thermal storage capacity. The geometrical parameters of shell and tube model are selected with an objective to develop an efficient and responsive LHS system that will be coupled with flat plate solar thermal system, which is previously designed and developed by Helvaci and Khan [44]. The outer diameter, length and thickness of the shell are 450 mm, 320 mm and 1 mm, respectively. The tube is connected with fins, each of 2 mm thickness. The fins are equidistant to each other. Commercial grade paraffin is selected as PCM for its high heat storage capacity, good chemical stability, no super-cooling, non-corrosiveness and low cost [6,45]. Water is made to flow in tube. The thermo-physical properties of paraffin are given in Table 1. Various configurations of shell and tube are examined, as depicted in Fig. 2. In all cases, the number of tube passes, fins number and fins geometry are selected to design a LHS system that is capable of melting entire mass of PCM within 10 h and with minimal reduction in thermal storage capacity. Likewise, the highest possible temperature attained by flat plate solar thermal system is in the range of 333.15 K [44]. To incorporate weather fluctuations, the selected range of inlet temperature of HTF is from 323.15 K to 343.15 K.

2.2. Governing equations

The governing equations to calculate the thermal performance and phase transition rate of PCM based LHS system are mass, momentum and energy conservation equations; which are described as follow:

Mass conservation:

$$\frac{\partial \rho}{\partial t} + \nabla \cdot (\rho \mathbf{u}) = 0 \tag{1}$$

Momentum conservation:

$$\frac{\partial (\rho \mathbf{u})}{\partial t} + \nabla \cdot (\rho \mathbf{u}\mathbf{u}) = -\nabla p + \nabla \cdot (\mu \nabla \mathbf{u}) + \mathbf{F} + S\mathbf{u} \tag{2}$$

Energy conservation:

$$\frac{\partial (\rho C_p T)}{\partial t} + \nabla \cdot (\rho C_p T \mathbf{u}) = \nabla \cdot (k \nabla T) + q \tag{3}$$

Table 1
Thermo-physical characteristics of paraffin [45].

Melting temperature, T_{pc}	41–44 °C or 314.15–317.15 K
Latent heat of fusion, L	255 (kJ/kg)
Specific heat, C_p	2.0 (kJ/kg K)
Thermal conductivity, k	0.2 (W/m K) (solid); 0.2 (W/m K) (liquid)
Density, ρ	800 (kg/m^3) (solid); 700 (kg/m^3) (liquid)
Dynamic viscosity, μ	0.008 (kg/m s)
Coefficient of thermal expansion, β	0.00259 (1/K)

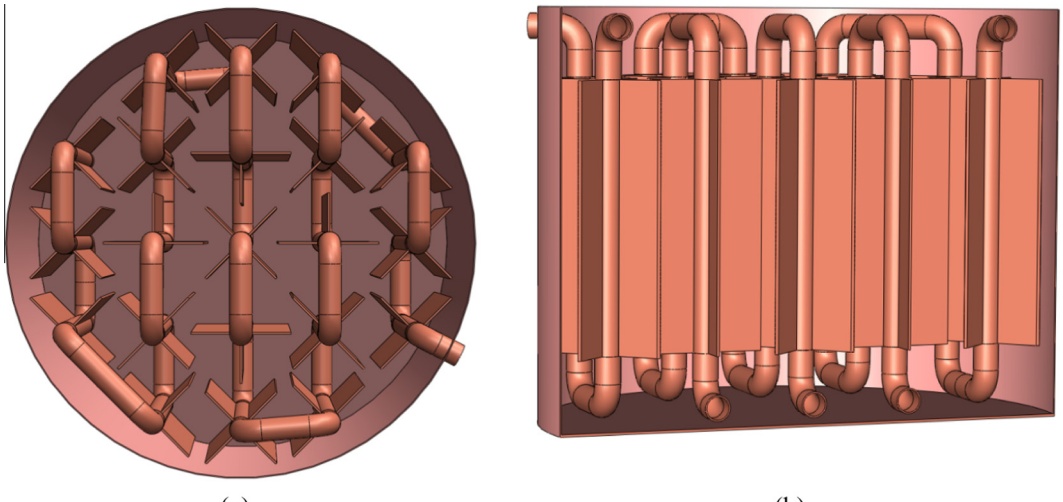

Fig. 1. Physical model of LHS system. (a) Top view and (b) cross section view.

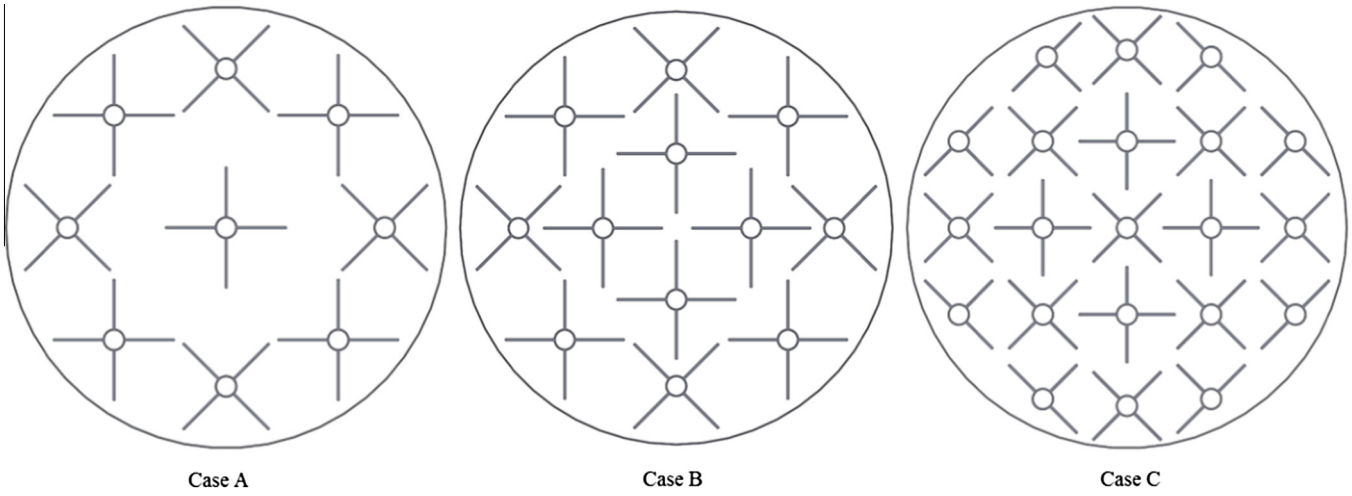

Fig. 2. Various configurations and orientations of shell and tube based LHS system.

where ρ, $\mathbf{u}$, p, μ, $\mathbf{F}$, S, C_p, k, T and q represents density (kg/m^3), velocity (m/s), pressure (Pa), dynamic viscosity (kg/m s), volume force (Pa/m), momentum source term, specific heat at constant pressure (kJ/kg K), thermal conductivity (W/m K), temperature (K) and heat source term (W/m^3), respectively. F in Eq. (2) can be estimated by using Boussinesq approximation [46,47] as follow:

$$\mathbf{F} = \rho \mathbf{g} \beta (T - T_{pc}) \tag{4}$$

where $\mathbf{g}$, β and T_{pc} shows gravitational acceleration (m/s^2), coefficient of thermal expansion (1/K) and phase change temperature (K), respectively. During phase transition, the enthalpy-porosity technique considers mushy zone as porous medium. The porosity and liquid fraction in each mesh element are assumed to be equivalent. In fully solidified mesh elements, the porosity is equal to zero. In order to reduce the velocity in solid region to zero, Kozeny-Carman equation is implemented to estimate the momentum source term S in Eq. (2), as follow [48,49]:

$$S = \frac{\kappa (1-f)^2}{(f^3 + \alpha)} \tag{5}$$

where κ represents morphology constant of mushy zone and α is a small value to avoid division by zero. In this study the values of κ and α are set to 10^7 and 10^{-4}, respectively. Further, the phase transition occurs in temperature interval of $T_s \leqslant T \leqslant T_l$. A smoothing function f is introduced which indicates the fraction of material in solid and liquid phase, as described below:

$$f = \begin{cases} 0 & T < T_s \\ \frac{T - T_s}{T_l - T_s} & T_s \leqslant T \leqslant T_l \\ 1 & T > T_l \end{cases} \tag{6}$$

where the indices s and l represent the solid and liquid phase of PCM, respectively. During phase transition interval, the specific enthalpy H can be defined as the combination of enthalpy in solid and liquid phase, as follow:

$$\rho H = f_s \rho_s H_s + f_l \rho_l H_l \tag{7}$$

To calculate effective specific heat capacity, Eq. (7) is differentiated with respect to temperature and simplified as follow:

$$C_p = \frac{\partial}{\partial T} \left[\frac{f_s \rho_s H_s + f_l \rho_l H_l}{\rho} \right] \tag{8}$$

$$C_p = \frac{1}{\rho} (f_s \rho_s C_{p,s} + f_l \rho_l C_{p,l}) + (H_l - H_s) \frac{\partial}{\partial T} \left[\frac{(f_l \rho_l - f_s \rho_s)}{2\rho} \right] \tag{9}$$

Eq. (9) indicates that effective specific heat capacity is the sum of sensible and latent heat components. The difference in enthalpies $H_l - H_s$ can be replaced with latent heat term L. Likewise, the thermal conductivity and density of PCM can be expressed as follow:

$$k = f_s k_s + f_l k_l \tag{10}$$

$$\rho = f_s \rho_s + f_l \rho_l \tag{11}$$

2.3. Initial and boundary conditions

As mentioned in Table 1, the phase transition temperature of PCM is 314.15 K. In the course of melting, the initial temperature of thermal storage unit is kept at room temperature at 298.15 K, which is less than melting temperature. It indicates that initially entire PCM is in solid phase. A constant boundary temperature is provided from HTF tube to PCM in shell, which ranges from 323.15 K to 343.15 K. The melting process starts at $t = 0$ s by supplying constant temperature from HTF tube walls. The exterior boundary of shell is assumed to be perfectly insulated.

2.4. Computational procedure and model validation

The governing equations are discretised by using finite element approach. In order to simplify the model, it is assumed that all tube passes transfer thermal energy to PCM at constant temperature T_h. The governing equations for HTF and PCM are simultaneously solved in entire computational domain due to coupled thermal energy transfer between HTF and PCM. Second order backward differentiation technique is employed for time stepping to check the relative tolerance. The relative tolerance is set to 0.001. The mesh independency and time stepping are validated by conducting a series of comparative investigations to find the influence of different mesh numbers and time steps on melt time. Case C from Fig. 2 is selected for this examination. Table 2 represent the impact of mesh numbers and time steps on the melt time. It is observed that when the time step is set to 1 min, the melt time for entire LHS system in case-II and case-III are 443 and 441, respectively. However, the difference in melt time for case-I and case-II is significant. Further, the melting fraction at a point, which is at 20 mm vertical distance from the outer boundary of central HTF tube, is illustrated in Fig. 3. It can be noticed from Fig. 3(b) that the melting fraction

Table 2
Validation of mesh independency and time stepping.

Case	Mesh numbers	HTF temperature (K)	Time step (min)	Melt time (min)	Percent error
I	28674	333.15	1	396	10.6
II	57861	333.15	1	443	–
III	61932	333.15	1	441	0.45
IV	57861	333.15	0.25	437	1.35
V	57861	333.15	0.5	452	2.03

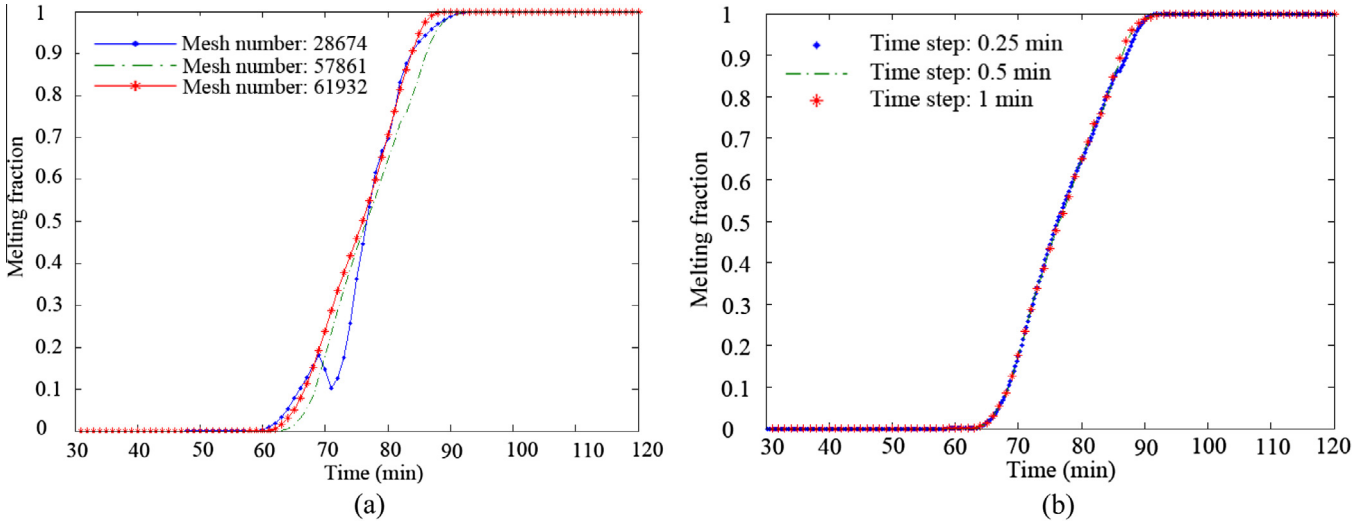

Fig. 3. (a) and (b) illustrates the mesh and time steps independency, respectively.

plots for all three time steps are almost identical. Therefore, the selected mesh numbers and time steps for this study are 57861 and 1 min, respectively.

The current computational model was validated by comparing the simulation results with experimental results which are reported by Liu and Groulx [50]. In their study, dodecanoic acid was employed as PCM in horizontal cylindrical container of 152.4 mm outer diameter. Copper pipe of 12.7 mm outer diameter was fitted through the centre of cylinder. Four fins were connected to copper pipe, each at 90°. Water was utilised as HTF through copper pipe. For validation purpose, the computational model was simulated using geometrical configuration, PCM, initial and boundary conditions and mass flow rate of HTF as reported in [50]. Fig. 4 depicts that both numerical results and experimental results are in good agreement.

3. Results and discussion

3.1. Numbers and orientations of tube passes

Fig. 5 demonstrates the melting fraction of PCM in various geometrical orientations of LHS system. The inlet temperature of HTF is set to 333.15 K for investigating the effect of numbers of tube passes on melting rate. The number of tube passes in case A, B and C are 9, 12 and 21, respectively. With an increase in tube pass, the volume of PCM in shell is compromised by tube and fins. On the contrary, it will increase the effective surface area for heat transfer and thus the low thermal conductivity of PCM can be improved. As a result, the melting rate of PCM can be significantly enhanced by increasing the tube passes.

In case A, the geometric orientation depicts that the tube passes are widely apart. It can be noticed that the tube pass at the centre and the tube passes near the boundary of shell are afar. Therefore, due to low thermal conductivity of PCM, the heat transfer is not very intense in this region. Initially, the melting process is dominated by conduction. It can be noticed from Fig. 5 that only 65.75% of PCM is melted after 5 h of heat transfer. With an increase in liquid percentage of PCM, the heat transfer is now dominated by convection. Further, the melting rate is reduced due to lack of conduction heat transfer. It can be observed that the liquid percentage of PCM is 95.45% and 99% after 10 h and 15 h of heat transfer, respectively. Likewise, even after 20 h, the PCM is not completely melted.

In case B, the surface area for heat transfer is increased by adding three more tube passes. Similar to case-A, the melting process is initially dominated by conduction. It is observed that after 4 h of heat transfer only 71.85% of PCM is in liquid phase. Convection dominates the heat transfer now and thus the melting rate reduces, as the liquid percentage of PCM is 96.07% and 99.5% after 8 h and 12 h, respectively. In case B, the entire PCM is melted in 15 h of continuous heat transfer.

In case C, the surface area for heat transfer is enhanced by increasing the number of tube passes to 21. In this case, the heat transfer is highly dominated by conduction as it can be seen that a huge percentage of PCM is melted within 3 h. It is noticed that the liquid percentage of PCM is 84%, 94.2% and 98.25% after 3 h, 4 h and 5 h of heat transfer, respectively. The entire PCM is melted in 7.5 h.

As depicted in Fig. 5, the melting rate for case C is significantly higher than case A and case B. It is noticed that due to higher effective surface area for heat transfer, the melt time for case C is about half as compared to case B. Also, due to the increase in tube passes, the heat transfer is dominated by conduction and therefore, the melting rate is improved significantly.

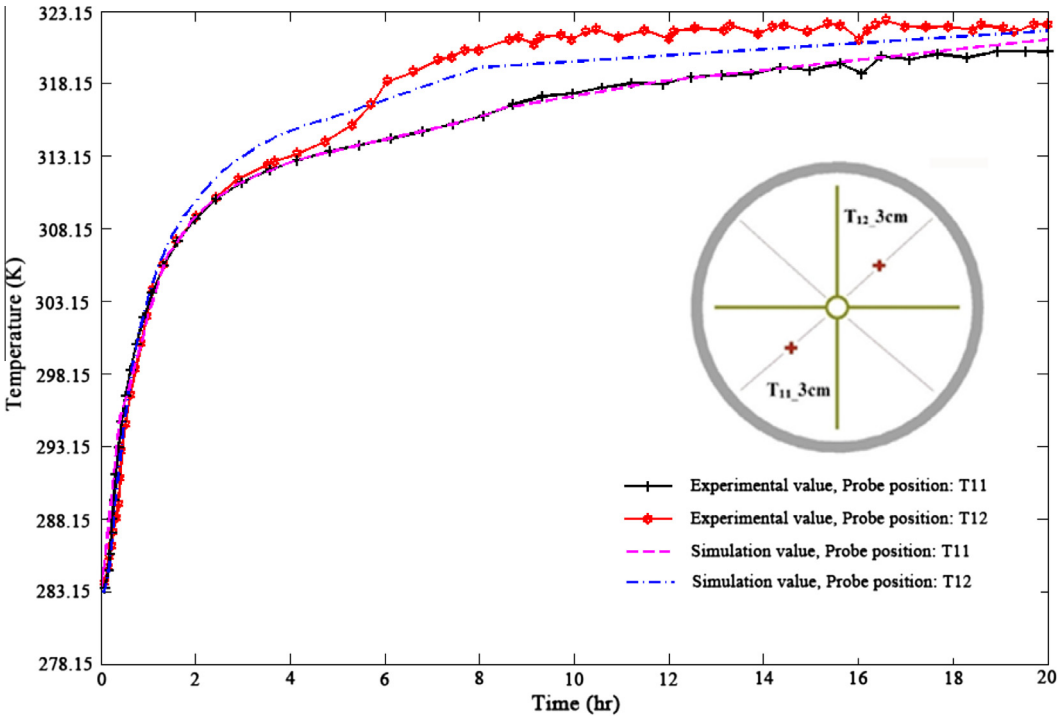

Fig. 4. Comparison of temperature profiles to validate numerical model with experimental results from [50]. For all cases, the inlet temperature and flow rate of HTF were set to 323.15 K and 1 L/min, respectively.

3.2. Longitudinal fins geometry

Fins geometry plays a significant role in enhancing the thermal performance of LHS system. Fig. 6 represents the effect of various fins lengths on melting fraction and temperature distribution in LHS system. Heat is transferred to LHS system for 4 h at inlet temperature of 333.15 K. The influence of various fins lengths ranging from 12.7 mm to 38.10 mm is investigated. Due to an increase in surface area, the thermal conduction enhances and consequently overall heat transfer improves. It is evident from Fig. 6 that the temperature distribution in entire system for case (d) is significantly better than other cases. After 4 h of heat transfer, the liquid fractions for case (a), (b), (c) and (d) are noted to be 59.2%, 72.98%, 83.86% and 94.66%, respectively.

It can be observed from Fig. 7 that as compared to case (a), the total melting time for case (e), (g) and (i) is reduced by 35.45%, 47.01% and 57.32%, respectively. However, it is noticed that the thermal storage capacity is reduced by increasing the fins length. It is noted that the thermal storage capacity for case (i) is 1.94% lesser than case (a). Due to higher melting rate, case (i) is selected for further investigations in this article.

Fig. 8 illustrates the impact of fins thickness on melting fraction and temperature distribution in LHS system. The HTF temperature is set to 333.15 K and the system is charged for 4 h. The effects of different fins thickness ranging from 1 mm to 5 mm are examined. It can be noticed from Fig. 8 that the melting fraction for all cases are almost similar after 4 h of heat transfer. The liquid fraction for case (a), (b), (c) and (d) are recorded to be 94.58%, 94.66%, 94.74% and 94.75%, respectively. Likewise, the fins thickness has minimal influence on the temperature distribution.

Fig. 9 represents the total melting time and variation in thermal storage capacity for all cases. It can be noticed that the total melting time for case (e), case (g) and case (i) is reduced by 10.25%, 13.25% and 16.45% as compared to case (a), respectively. However, an increase in fins thickness can limit the volume for PCM and therefore the thermal storage capacity of LHS system can be compromised. As shown in Fig. 9, the thermal storage capacity for case (i) is reduced by 5.7% as compared to case (a), respectively.

3.3. Shell, tube and fins materials

The low thermal conductivity of PCM can be boosted by employing higher thermal conductive shell, tube and fins. High thermal conductive materials play a vital role in improving the thermal performance of LHS system. In order to analyse the influence of material on thermal performance, the following materials are examined: steel AISI 4340, cast iron, tin, nickel, aluminium 6063, aluminium and copper. The inlet temperature of HTF is kept constant at 333.15 K for all materials. Table 3 represents the percent liquid fraction and complete melting time of PCM against various materials. It is observed that as the thermal conductivity of material increases, the heat transfer rate between HTF and PCM increases and therefore the melting rate of PCM strengthens. Due to higher thermal conductivity of copper, the required melting time for PCM is reduced by 23.68% as compared to steel AISI 4340. Likewise, aluminium and aluminium 6063 presents a good thermal performance, as the melting time is reduced by 18.84% and 17.88% comparing to cast iron, respectively. It is evident from Table 3 that copper and aluminium are the suitable materials to be employed as shell, tube and fins material.

3.4. Inlet temperature of HTF

In order to examine the influence of inlet temperature of HTF on melting rate and increase in enthalpy of LHS system, various inlet temperatures are investigated ranging from 323.15 K to 343.15 K. An increase in inlet temperature of HTF produces higher temperature difference between PCM and HTF and consequently the heat transfer rate is accelerated. Due to an increase in heat transfer, the melting rate of PCM is enhanced, as shown in Fig. 10. It is evident that LHS system in case (d) is at notable higher temperature compared to case (a) and thus majority of the PCM is either in

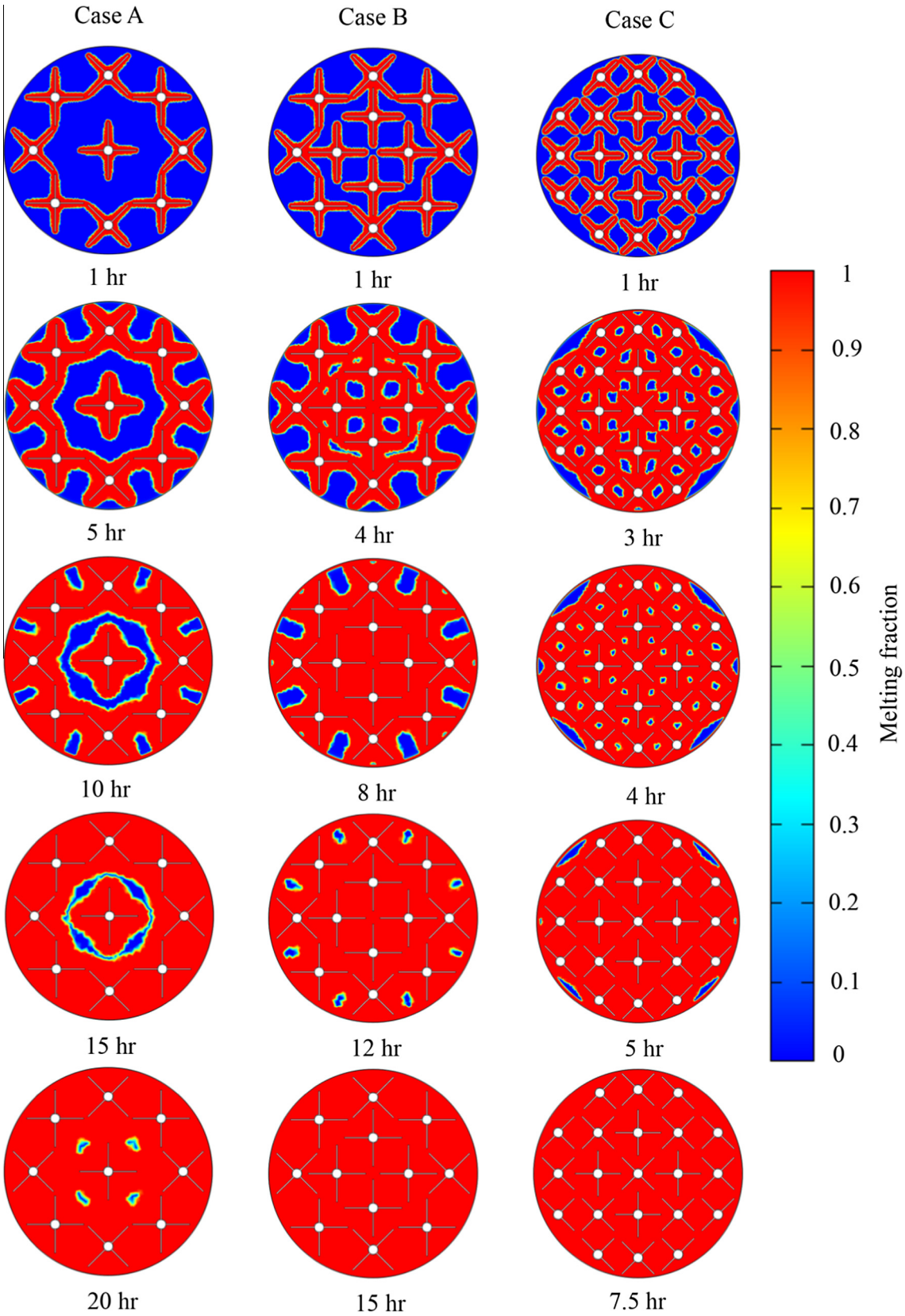

Fig. 5. Liquid fraction for all the three cases at inlet temperature of 333.15 K.

liquid state or mushy zone. After 4 h of heat transfer, the liquid fraction for case (a), (b) (c) and (d) are noted to be 66.71%, 92.93%, 93.65% and 99.55%, respectively. Fig. 11 illustrates that the total melting time is reduced by 42.8%, 52.4% and 68.8% as the inlet temperature of HTF is increased from 323.15 K to 328.15 K, 333.15 K and 343.15 K, respectively. Also, due to the

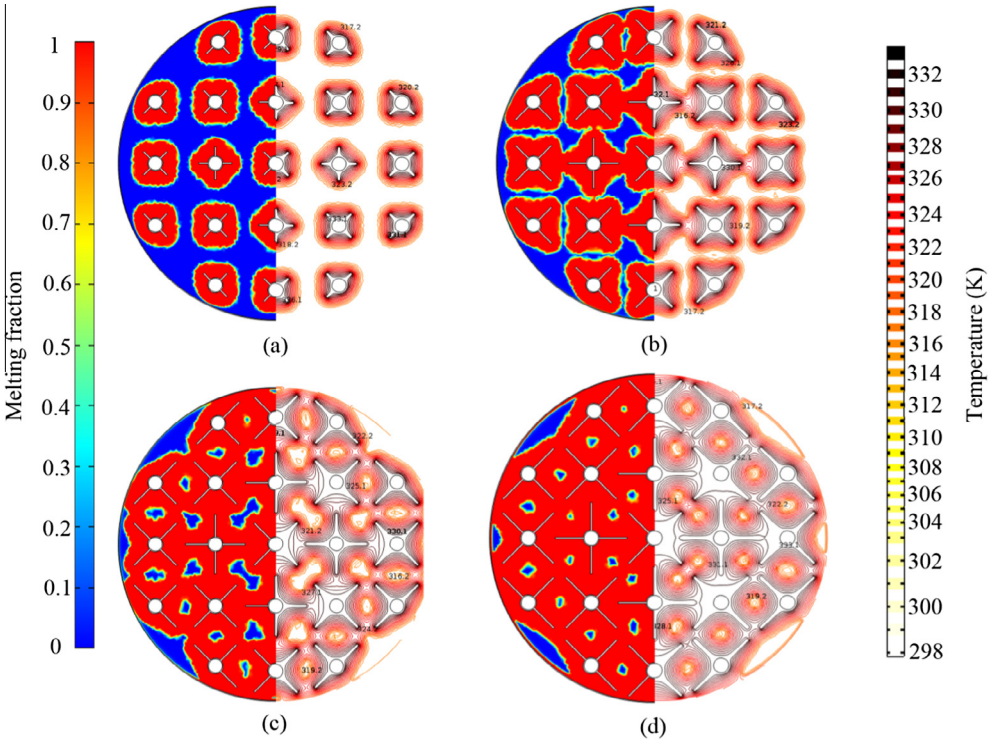

Fig. 6. Influence of fins length on melting fraction and temperature contours after charging for 4 h. Fins thickness is set to 2 mm for all cases. (a) Fins length = 12.7 mm, (b) fins length = 25.4 mm, (c) fins length = 31.75 mm and (d) fins length = 38.10 mm.

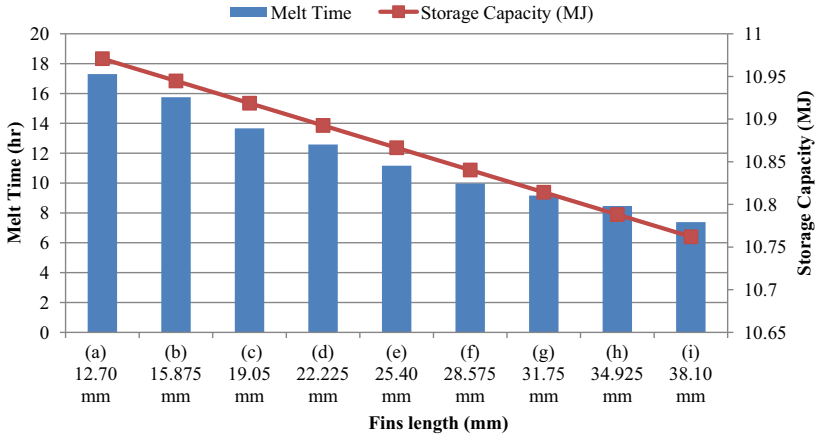

Fig. 7. Effects of fins length on total melt time and thermal storage capacity.

increase in inlet temperature, the sensible enthalpy of the system is also augmented, which results in enhancing the overall thermal storage capacity. Fig. 11 shows that the enthalpy of LHS system for case (c), case (e) and case (i) is increased by 4.52%, 9.03% and 18.06% as compared to case (a), respectively.

4. Conclusions

In this article, a computational model is employed to examine the thermal performance of novel shell and tube configuration based LHS system. Parametric investigation is conducted to inspect the improvement in thermal performance due to the number of tube passes, length and thickness of longitudinal fins, materials for shell, tube and fins, and inlet temperature of HTF. The augmented thermal behaviour of LHS system can attain both time and economic benefits, along with extensive and sustainable employment in both domestic and industrial applications. From the numerical results the following conclusions are reached:

- It is observed that as the number of tube passes is increased from 9 to 21, the thermal performance of the LHS system is significantly enhanced. This is due to the fact that the thermal conductivity and effective surface area for heat transfer increases by increasing the number of tubes. The heat transfer is dominated by conduction heat transfer and therefore the required melting time for 21 number of tube passes is reduced by 48.5% to that of 12 tube passes.
- The geometry of the fins plays a vital role in improving the thermal performance of LHS system. It is noticed that as the length

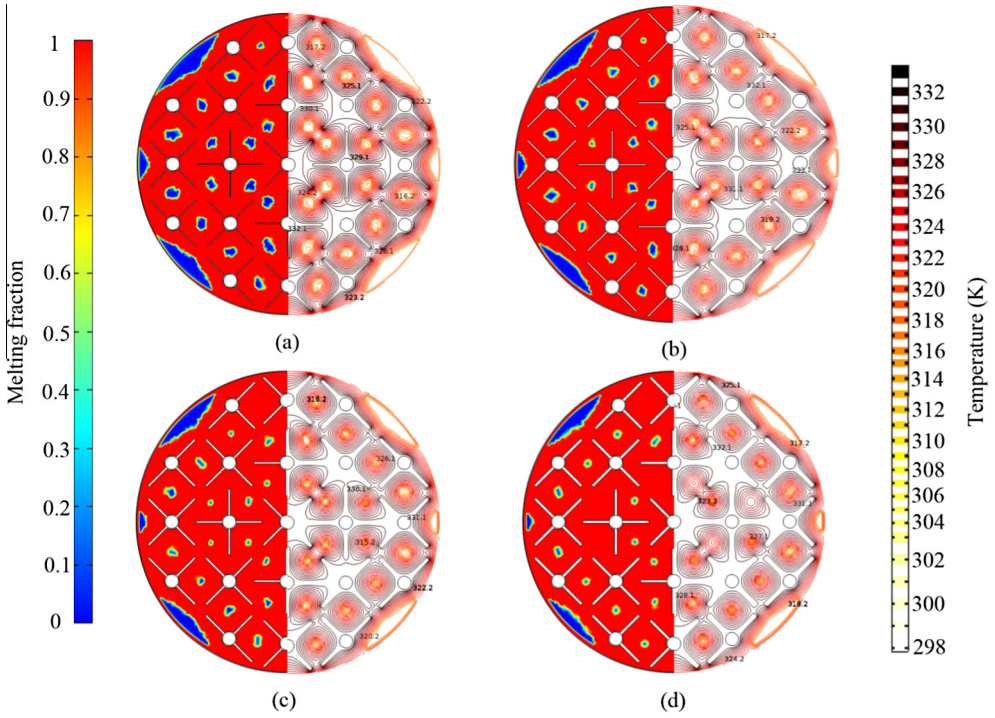

Fig. 8. Influence of fins thickness on melting fraction and temperature contours after charging for 4 h. (a) fins thickness = 1 mm, (b) fins thickness = 2 mm, (c) fins thickness = 3 mm and (d) fins thickness = 4 mm.

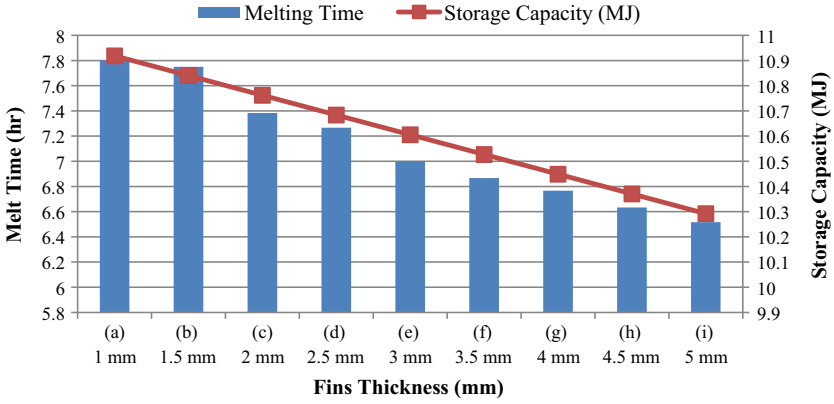

Fig. 9. Effects of fins thickness on total melt time and thermal storage capacity.

Table 3
Effect of shell, tube and fins material on melting rate of LHS system.

Materials	Thermal conductivity (W/(m K)) [51]	Percent liquid fraction					Complete melting time (h)
		2 h	4 h	6 h	8 h	10 h	
Steel AISI 4340	44.5	63.92	85.23	95.53	99.25	100	9.67
Cast iron	50	65.06	86.23	96.19	99.46	100	9.34
Tin	67	67.30	87.69	97.30	99.71	100	8.92
Nickel	90	68.57	88.32	97.78	99.85	100	8.75
Aluminium 6063	201	72.77	92.19	99.08	100		7.67
Aluminium	238	73.05	92.68	99.15	100		7.58
Copper	400	73.63	93.69	99.34	100		7.38

of the fins is increased from 12.7 mm to 38.10 mm, the thermal conductivity of the system improved and consequently the heat transfer between HTF and PCM. The melting time is reduced by 57.32% as the length of the fins is increased from 12.7 mm to 38.10 mm.

- Fins thickness influences the melting time of the PCM. However, it is observed that increase in fins length has more prominent effects on thermal performance than fins thickness. Also, the thermal storage capacity of system is decreased by 5.7% as the fins thickness is increased from 1 mm to 5 mm.

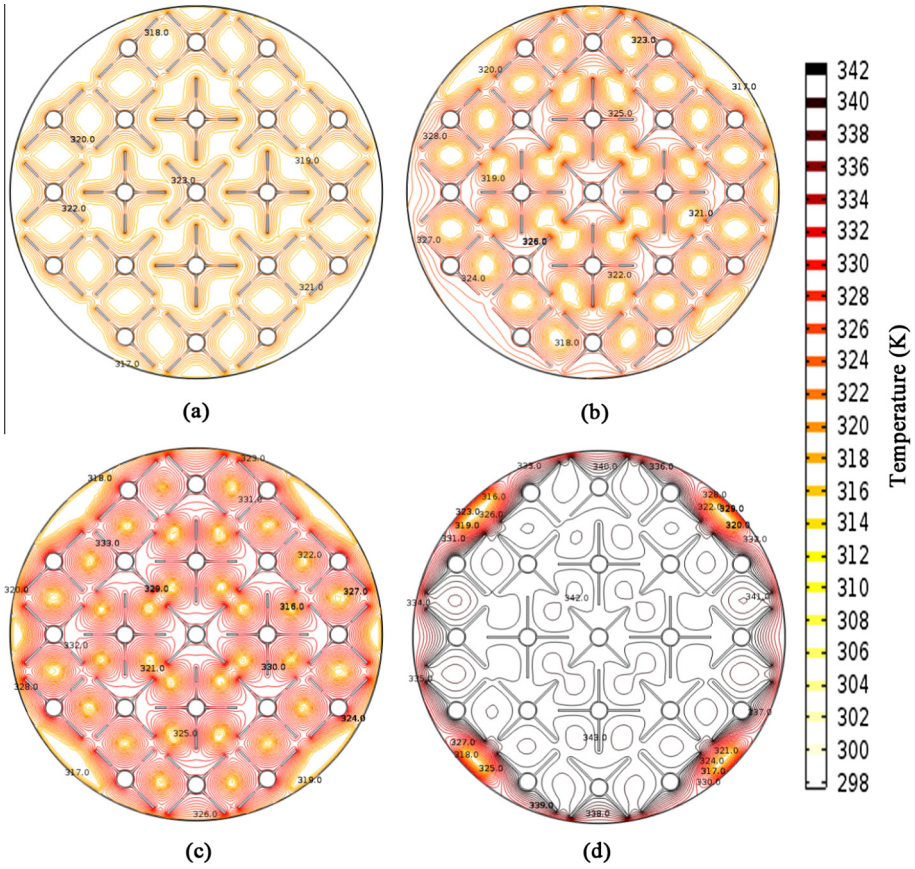

Fig. 10. Temperature contours of LHS system after 4 h of heat transfer. Various inlet temperatures of HTF are (a) 323.15 K, (b) 328.15 K, (c) 333.15 K and (d) 343.15 K.

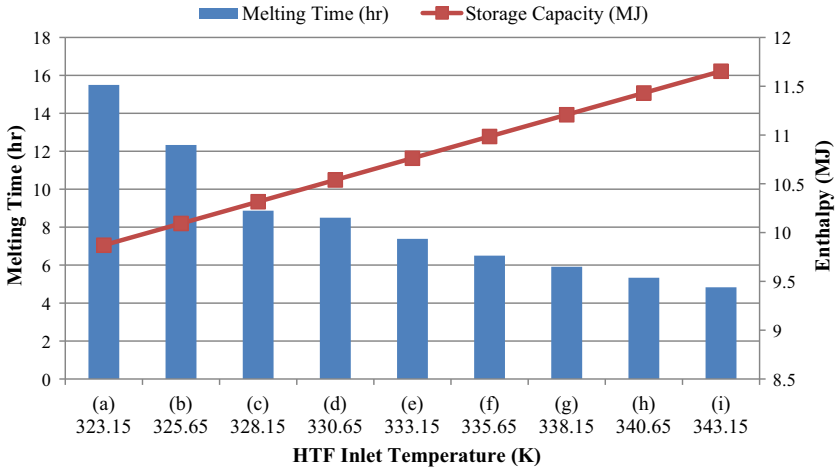

Fig. 11. Impact of inlet temperature of HTF on melting time and thermal storage capacity.

- Shell, tubes and fins material has significant effect on the thermal performance. It is recommended to use high thermal conductive material, which is compatible with PCM. It was observed that copper, aluminium and aluminium 6063 has considerably better thermal performance with paraffin as compared to steel AISI 4340.
- The enthalpy and melting rate is augmented by increasing the inlet temperature of HTF from 323.15 K to 343.15 K. Due to increase in inlet temperature, the sensible enthalpy increases and therefore the overall system thermal storage capacity is increased by 18.06%. Likewise, the melting time is reduced by 68.8%.

Acknowledgment

This project is match funded by Bournemouth University, UK and National University of Sciences and Technology (NUST), Pakistan within their international research collaboration initiative. The authors would like to acknowledge both financial and in-kind support provided by both universities.

References

[1] Farid MM, Khudhair AM, Razack SAK, Al-Hallaj S. A review on phase change energy storage: materials and applications. Energy Convers Manage 2004;45:1597–615.
[2] Sharma A, Tyagi V, Chen C, Buddhi D. Review on thermal energy storage with phase change materials and applications. Renew Sustain Energy Rev 2009;13:318–45.
[3] Dhaidan NS, Khodadadi J. Melting and convection of phase change materials in different shape containers: a review. Renew Sustain Energy Rev 2015;43:449–77.
[4] Archibold AR, Gonzalez-Aguilar J, Rahman MM, Goswami DY, Romero M, Stefanakos EK. The melting process of storage materials with relatively high phase change temperatures in partially filled spherical shells. Appl Energy 2014;116:243–52.
[5] Jegadheeswaran S, Pohekar SD. Performance enhancement in latent heat thermal storage system: a review. Renew Sustain Energy Rev 2009;13:2225–44.
[6] Khan Z, Khan Z, Ghafoor A. A review of performance enhancement of PCM based latent heat storage system within the context of materials, thermal stability and compatibility. Energy Convers Manage 2016;115:132–58.
[7] Salunkhe PB, Shembekar PS. A review on effect of phase change material encapsulation on the thermal performance of a system. Renew Sustain Energy Rev 2012;16:5603–16.
[8] Liu C, Rao Z, Zhao J, Huo Y, Li Y. Review on nanoencapsulated phase change materials: preparation, characterization and heat transfer enhancement. Nano Energy 2015;13:814–26.
[9] Giro-Paloma J, Martínez M, Cabeza LF, Fernández AI. Types, methods, techniques, and applications for Microencapsulated Phase Change Materials (MPCM): a review. Renew Sustain Energy Rev 2016;53:1059–75.
[10] Fan L-W, Zhu Z-Q, Xiao S-L, Liu M-J, Lu H, Zeng Y, et al. An experimental and numerical investigation of constrained melting heat transfer of a phase change material in a circumferentially finned spherical capsule for thermal energy storage. Appl Therm Eng 2016;100:1063–75.
[11] Zhang H, Baeyens J, Degrève J, Cáceres G, Segal R, Pitié F. Latent heat storage with tubular-encapsulated phase change materials (PCMs). Energy 2014;76:66–72.
[12] Tian B, Yang W, Luo L, Wang J, Zhang K, Fan J, et al. Synergistic enhancement of thermal conductivity for expanded graphite and carbon fiber in paraffin/EVA form-stable phase change materials. Sol Energy 2016;127:48–55.
[13] Liu Z, Zhang Y, Hu K, Xiao Y, Wang J, Zhou C, et al. Preparation and properties of polyethylene glycol based semi-interpenetrating polymer network as novel form-stable phase change materials for thermal energy storage. Energy Build 2016;127:327–36.
[14] Li R, Zhu J, Zhou W, Cheng X, Li Y. Thermal properties of sodium nitrate-expanded vermiculite form-stable composite phase change materials. Mater Des 2016;104:190–6.
[15] Feng L, Wang C, Song P, Wang H, Zhang X. The form-stable phase change materials based on polyethylene glycol and functionalized carbon nanotubes for heat storage. Appl Therm Eng 2015;90:952–6.
[16] Silakhori M, Fauzi H, Mahmoudian MR, Metselaar HSC, Mahlia TMI, Khanlou HM. Preparation and thermal properties of form-stable phase change materials composed of palmitic acid/polypyrrole/graphene nanoplatelets. Energy Build 2015;99:189–95.
[17] Zeng J-L, Gan J, Zhu F-R, Yu S-B, Xiao Z-L, Yan W-P, et al. Tetradecanol/expanded graphite composite form-stable phase change material for thermal energy storage. Sol Energy Mater Sol Cells 2014;127:122–8.
[18] Khodadadi J, Fan L, Babaei H. Thermal conductivity enhancement of nanostructure-based colloidal suspensions utilized as phase change materials for thermal energy storage: a review. Renew Sustain Energy Rev 2013;24:418–44.
[19] Fan L, Khodadadi J. Thermal conductivity enhancement of phase change materials for thermal energy storage: a review. Renew Sustain Energy Rev 2011;15:24–46.
[20] Liu L, Su D, Tang Y, Fang G. Thermal conductivity enhancement of phase change materials for thermal energy storage: a review. Renew Sustain Energy Rev 2016;62:305–17.
[21] Kamkari B, Shokouhmand H. Experimental investigation of phase change material melting in rectangular enclosures with horizontal partial fins. Int J Heat Mass Transf 2014;78:839–51.
[22] Kalbasi R, Salimpour MR. Constructal design of horizontal fins to improve the performance of phase change material rectangular enclosures. Appl Therm Eng 2015;91:234–44.
[23] Ren Q, Chan CL. GPU accelerated numerical study of PCM melting process in an enclosure with internal fins using lattice Boltzmann method. Int J Heat Mass Transf 2016;100:522–35.
[24] Li Z, Wu Z-G. Analysis of HTFs, PCMs and fins effects on the thermal performance of shell–tube thermal energy storage units. Sol Energy 2015;122:382–95.
[25] Darzi AAR, Jourabian M, Farhadi M. Melting and solidification of PCM enhanced by radial conductive fins and nanoparticles in cylindrical annulus. Energy Convers Manage 2016;118:253–63.
[26] Yuan Y, Cao X, Xiang B, Du Y. Effect of installation angle of fins on melting characteristics of annular unit for latent heat thermal energy storage. Sol Energy 2016;136:365–78.
[27] Caron-Soupart A, Fourmigué J-F, Marty P, Couturier R. Performance analysis of thermal energy storage systems using phase change material. Appl Therm Eng 2016;98:1286–96.
[28] Agyenim F, Eames P, Smyth M. A comparison of heat transfer enhancement in a medium temperature thermal energy storage heat exchanger using fins. Sol Energy 2009;83:1509–20.
[29] Rathod MK, Banerjee J. Thermal performance enhancement of shell and tube Latent Heat Storage Unit using longitudinal fins. Appl Therm Eng 2015;75:1084–92.
[30] Luo K, Yao F-J, Yi H-L, Tan H-P. Lattice Boltzmann simulation of convection melting in complex heat storage systems filled with phase change materials. Appl Therm Eng 2015;86:238–50.
[31] Esapour M, Hosseini M, Ranjbar A, Pahamli Y, Bahrampoury R. Phase change in multi-tube heat exchangers. Renewable Energy 2016;85:1017–25.
[32] Vyshak N, Jilani G. Numerical analysis of latent heat thermal energy storage system. Energy Convers Manage 2007;48:2161–8.
[33] Tao Y, He Y, Qu Z. Numerical study on performance of molten salt phase change thermal energy storage system with enhanced tubes. Sol Energy 2012;86:1155–63.
[34] Li Z, Tang G, Wu Y, Zhai Y, Xu J, Wang H, et al. Improved gas heaters for supercritical CO_2 Rankine cycles: considerations on forced and mixed convection heat transfer enhancement. Appl Energy 2016;178:126–41.
[35] Tao Y, He Y. Effects of natural convection on latent heat storage performance of salt in a horizontal concentric tube. Appl Energy 2015;143:38–46.
[36] Wang W-W, Wang L-B, He Y-L. Parameter effect of a phase change thermal energy storage unit with one shell and one finned tube on its energy efficiency ratio and heat storage rate. Appl Therm Eng 2016;93:50–60.
[37] Tiari S, Qiu S, Mahdavi M. Discharging process of a finned heat pipe–assisted thermal energy storage system with high temperature phase change material. Energy Convers Manage 2016;118:426–37.
[38] Al-Abidi AA, Mat S, Sopian K, Sulaiman MY, Mohammad AT. Experimental study of melting and solidification of PCM in a triplex tube heat exchanger with fins. Energy Build 2014;68:33–41.
[39] Mat S, Al-Abidi AA, Sopian K, Sulaiman MY, Mohammad AT. Enhance heat transfer for PCM melting in triplex tube with internal–external fins. Energy Convers Manage 2013;74:223–36.
[40] Hosseini M, Ranjbar A, Rahimi M, Bahrampoury R. Experimental and numerical evaluation of longitudinally finned latent heat thermal storage systems. Energy Build 2015;99:263–72.
[41] Seddegh S, Wang X, Henderson AD. A comparative study of thermal behaviour of a horizontal and vertical shell-and-tube energy storage using phase change materials. Appl Therm Eng 2016;93:348–58.
[42] Kibria M, Anisur M, Mahfuz M, Saidur R, Metselaar I. Numerical and experimental investigation of heat transfer in a shell and tube thermal energy storage system. Int Commun Heat Mass Transf 2014;53:71–8.
[43] Wang W-W, Zhang K, Wang L-B, He Y-L. Numerical study of the heat charging and discharging characteristics of a shell-and-tube phase change heat storage unit. Appl Therm Eng 2013;58:542–53.
[44] Helvaci H, Khan ZA. Mathematical modelling and simulation of multiphase flow in a flat plate solar energy collector. Energy Convers Manage 2015;106:139–50.
[45] Rubitherm® Technologies GmbH. <http://www.rubitherm.eu/en/>; 2016.
[46] Mohamad A, Kuzmin A. A critical evaluation of force term in lattice Boltzmann method, natural convection problem. Int J Heat Mass Transf 2010;53:990–6.
[47] Gray DD, Giorgini A. The validity of the Boussinesq approximation for liquids and gases. Int J Heat Mass Transf 1976;19:545–51.
[48] Nield DA, Bejan A. Convection in porous media. Springer Science & Business Media; 2006.
[49] Tiari S, Qiu S, Mahdavi M. Numerical study of finned heat pipe-assisted thermal energy storage system with high temperature phase change material. Energy Convers Manage 2015;89:833–42.
[50] Liu C, Groulx D. Experimental study of the phase change heat transfer inside a horizontal cylindrical latent heat energy storage system. Int J Therm Sci 2014;82:100–10.
[51] MatWeb. <http://www.matweb.com/index.aspx>; 2016.